

Ferroelectricity in BiMnO₃ Thin Films

Yun-Peng Wang,^{1,2} J. N. Fry,¹ and Hai-Ping Cheng^{1,2*}

¹*Department of Physics, University of Florida, Gainesville, Florida 32611, USA*

²*Quantum Theory Project, University of Florida, Gainesville, Florida 32611, USA*

The existence of ferroelectricity in BiMnO₃ has been a long-standing question for both experimentalists and theorists. In addition to a highly distorted bulk structure, the ionic crystal planes cause a large roughness in thin films that makes it extremely difficult to nail down the physical mechanisms underlying a possible ferroelectric-ferromagnetic phase. We approach the problem by including the substrate explicitly to study the polarization. With this model, we investigate mono-, di-, and trilayer BiMnO₃ thin films on SrTiO₃ substrates. We find that thin film systems have both strong ferromagnetism and strong ferroelectricity. Substrate constraints weaken the competition between displacements induced by stereochemically active Bi-6s² lone pairs and by Jahn-Teller distortions around Mn ions found in the bulk, such that the sum of off-center displacements of Bi ions in bulk BiMnO₃ nearly cancel. In BiMnO₃ thin films, in contrast, all Bi ions displace roughly in parallel, resulting in a strongly polar structure. We also find spontaneous charge disproportionation of Mn ion pairs in BiMnO₃ thin films.

Keywords: multiferroic; BiMnO₃; epitaxial substrate constraint

Introduction. Multiferroic materials, exhibiting magnetic and ferroelectric orders simultaneously, have generated intense interest due to the rich physics of magneto-electric coupling and promise in spintronics applications [1–4]. Although magnetic and ferroelectric order parameters are predicted to be difficult to manifest simultaneously [5], several series of compounds with multiferroic properties were discovered in the last decade and have been classified according to the origin of ferroelectric order [1–4]. Most multiferroic materials unfortunately exhibit only weak magnetism, due to canted antiferromagnetic or cycloidal spiral spin order.

Bismuth manganite, BiMnO₃, with a highly distorted perovskite structure, was once regarded as the unique multiferroic compound presenting both ferromagnetic and ferroelectric orders. Although a C2 space group model was proposed in early studies [6, 7], Belik *et al.* [8] and Montanari *et al.* [9] have argued that bulk BiMnO₃ fits to A centrosymmetric C2/c space group that forbids ferroelectric order. Ferromagnetic order in BiMnO₃ is attributed to the three-dimensional orbital ordering [6–8], and the magnetic structure can be affected by pressure [10, 11]. The ferromagnetic Curie temperature is around 100 K [8, 9]. Each Mn³⁺ ion carries a magnetic moment of 3.92 μ_B , or close to 4 μ_B , at low temperatures [8]. A magneto-electric coupling is manifested by a change in the dielectric constant induced by magnetic fields at the Curie temperature [12]. Ferroelectric order in bulk BiMnO₃ was discussed in the literature [6–9, 13, 14]. Inversion symmetry breaking is expected due to the stereochemically active lone pairs 6s² of Bi³⁺, which make it possible to form cooperative ferroelectric distortions; this mechanism is the origin of ferroelectricity in BiFeO₃ [15]. Measurements of ferroelectric polarization in bulk BiMnO₃ were hampered by the high leakage currents of polycrystalline samples [12], and the measured polarization in bulk BiMnO₃ [13, 14] was attributed to extrinsic

factors. Ferroelectricity in bulk BiMnO₃ thus remains in question.

BiMnO₃ epitaxial thin films have also been investigated for ferroelectricity. Substrates can stabilize single crystal structure of BiMnO₃ [16]. More interestingly, the strain imposed by substrates can change the ferroelectric properties of perovskite materials [17]. Again, some BiMnO₃ thin film samples show ferroelectric properties [13, 18–22], while other studies supported an absence of ferroelectricity in BiMnO₃ thin films [23, 24]

Difficulties in synthesizing high-quality BiMnO₃ samples make theoretical studies using density functional theory (DFT) indispensable. Ferroelectric instability in BiMnO₃ was investigated based on local spin density approximation (LSDA) calculations [25]. The stability of the centrosymmetric C2/c phase over the C2 phase was confirmed using LSDA with an on-site Hubbard Coulomb correction (LSDA+*U*) [26] and BiMnO₃ was predicted to be nonpolar under compressive or tensile strain [27]. Recent studies showed that LSDA+*U* and GGA+*U* (GGA: generalized gradient approximation) fail to reproduce the structural distortions and energy gap in C2/c BiMnO₃. The strength of Jahn-Teller distortions around Mn³⁺ ions is heavily underestimated even with the Hubbard Coulomb correction on Mn-*d* orbitals [28]. The LSDA+*U* and GGA+*U* energy gap, 0.3–0.5 eV, is also substantially smaller than the 0.9 eV found in experiment [29]. A recent calculation using the modified Becke-Johnson exchange potential by Tran and Blaha [30] gives a 0.75 eV energy gap [31]. Hybrid functionals are capable of reproducing the structural distortion, but overestimate the energy gap [32]. Epitaxial phases of BiMnO₃ were also studied theoretically in [27, 32], in which substrate effects were simulated using constraints on the in-plane lattice vectors. The rationale behind this approach is that thin films satisfying the epitaxial relation with respect to the substrates are thick enough so that a periodic bulk de-

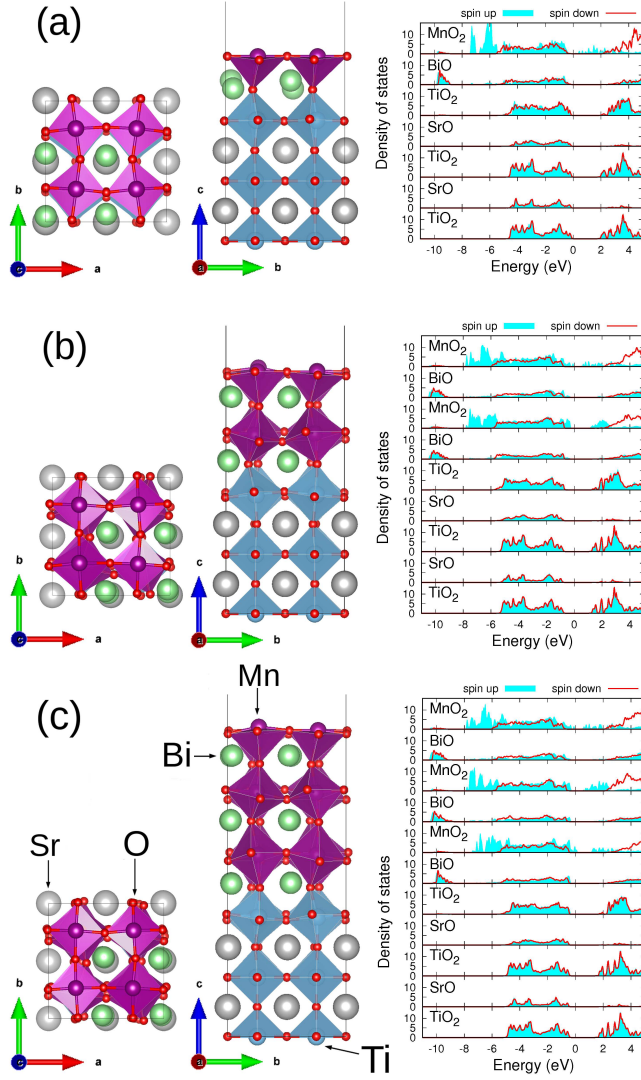


FIG. 1. Atomic structures and layer-projected density of states of (a) monolayer, (b) bilayer and (c) trilayer BiMnO_3 thin films on SrTiO_3 substrates.

scription is appropriate. The C2/c phase was found to be the ground state for the in-plane lattice constant between 3.75 and 4 Å, and thus ferroelectric order is forbidden.[32]

The aim of this study is to address the difficult issue of ferroelectricity in BiMnO_3 epitaxial thin films and to unveil the interplay among structure, electronic and magnetic structure. To accomplish this goal, we first establish a DFT-based theoretical approach including both Hubbard Coulomb and exchange corrections (see Supplementary Material section I.A) that proves capable of providing a satisfactory description of the physical properties of bulk BiMnO_3 . The Hubbard exchange term, overlooked in previous theoretical studies, plays a crucial role in describing noncollinear magnets [33], multiband metals [34, 35], Fe-based superconductors [36], and man-

ganites [37]. This is the first key that differentiates this work from previous theoretical studies. The second key is including explicitly the substrate instead of simulating the epitaxial condition merely by fixing the lateral size of the unit box. It is reported [20] that BiMnO_3 thin films lose the epitaxial constraint relation with respect to substrates when the thickness is larger than $\sim 10\text{nm}$. In ultrathin films, interface effects not seen in bulk form can be significant, such as the emergence of novel physical properties exhibited by perovskite superlattices and heterointerfaces [38–41].

Computational method. Calculations were carried out using the DFT with Hubbard Coulomb and exchange corrections (DFT+U+J) method. The two parameters U and J of this method were determined to reproduce the experimental properties of bulk BiMnO_3 . See Section I of Supplementary Material for more details.

For substrate material we chose SrTiO_3 , which is widely used in experiments [20, 42–44]. The ultrathin BiMnO_3 films are simulated using $\text{BiMnO}_3/\text{SrTiO}_3/\text{BiMnO}_3$ slabs in which five atomic-layer thick, TiO_2 -terminated SrTiO_3 serves as the substrate. A 2×2 pseudo-cubic supercell along the in-plane directions is used and the in-plane lattice

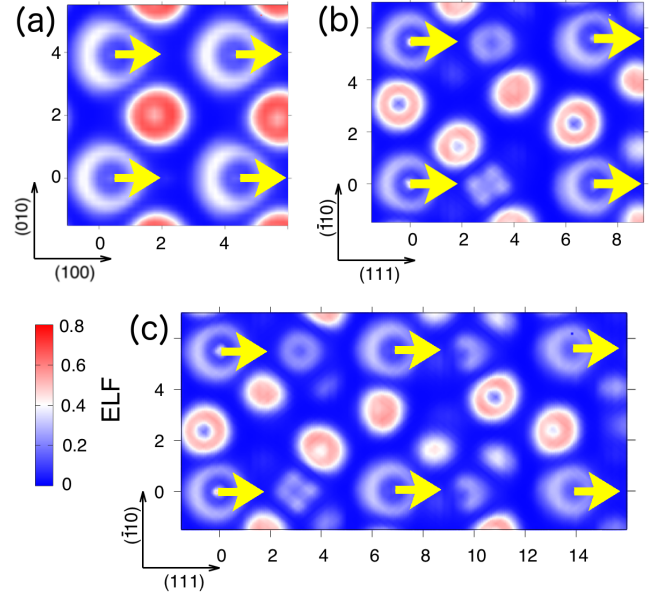


FIG. 2. ELF (electron localization function) of (a) monolayer, (b) bilayer, and (c) trilayer BiMnO_3 thin films. The ELF is plotted on a plane crossing the ions. In (a) the plane is parallel to the (100) and (010) directions. In (b) and (c) the plane is parallel to the (111) and $(\bar{1}10)$ directions. Bi ions at the surface appear at the right hand side of (b) and (c). The off-center displacements of Bi ions are denoted by arrows. The ELF around Bi ions loss spherical symmetry and Bi- $6s^2$ lone pairs are localized in the direction opposite to Bi off-center displacements. Other visible features in the ELF plot are contributed by oxygen.

constant in the central region is fixed at the SrTiO_3 substrate bulk value (3.905 Å). The epitaxial conditions imposed by the substrate are maintained during structural relaxation. The slab model is symmetric in the z -direction to maximally illuminate dipole-dipole interactions.

Results and discussion. Calculated magnetic and vibrational properties of bulk BiMnO_3 are in good agreement with experimental data. The detailed data are included in Section II of the Supplementary Material. The bulk is not ferroelectric, and our analysis shows a cancelation of dipole moments due to disordered Bi ion displacements, unlike in BiFeO_3 in which Bi displacements are aligned. The reason lies in the co-existence of stereochemically active $\text{Bi-}6s^2$ lone pairs and Jahn-Teller distortions around Mn ions. From this, we move on to examine thin film systems.

The atomic structures of the BiMnO_3 -substrate interfaces are obtained for monolayer, bilayer, and trilayer BiMnO_3 thin films on SrTiO_3 (Fig. 1). Structural results confirm the possible existence of ferroelectric order. We first examine the off-center displacements of Bi ions, which are the main driver necessary for ferroelectricity in BiMnO_3 . In a nutshell, Bi ions occupy the A-site of perovskite structures and are surrounded by twelve oxygens. Bi ions tend to exhibit off-center displacements due to their $6s^2$ lone pairs [45]. Among the four inequivalent Bi ions of a BiMnO_3 monolayer, two of them move along the pseudo-cubic (010) direction by 0.6 Å, and the other two along the (011) direction by 0.7 Å. For thicker BiMnO_3 films, Bi ions below the surface layer are shifted along the (111) direction by about 0.5 Å, while the displacement direction is between (111) and (001) for Bi ions at the surface layer. The most important observation here is that the displacements of Bi ions are roughly parallel to each other, which leads to a polar structure of BiMnO_3 thin films. This is a key finding of this work. The stereochemically active $\text{Bi-}6s^2$ lone pairs are illustrated by the electron localization function (ELF) [46]. ELF measures the extent of electron pair probability (see Supplementary Material Section I.C.), and was employed for illustrating lone pairs. The ELF of BiMnO_3 thin films is shown in Fig. 2, in which the off-center displacements of Bi ions are denoted by arrows. The ELF around each Bi ion shows a loss of spherical symmetry, indicating that the spatial distribution of $6s^2$ lone pairs is accumulated in the direction opposite the ion displacement.

Band structure and density of states analysis shows that energy gaps for mono-, bi-, and trilayer systems are 0.20, 0.40, and 0.20 eV respectively. Our calculations also show that these three BiMnO_3 systems are ferromagnetic, and we thus conclude that BiMnO_3 thin films on SrTiO_3 are multiferroic. Detailed analysis of magnetic moments will be given later.

In order to understand the mechanism for the polar structure of BiMnO_3 films, we compare off-center dis-

placements of Bi ions with those in bulk BiMnO_3 and bulk BiFeO_3 (detailed data are in Section IIA Supplementary Material). In bulk C2/c BiMnO_3 , Bi displacements are close to the pseudo-cubic (011) and (0 $\bar{1}$ 1) directions, and they cancel with each other, for a nonpolar structure. In BiMnO_3 thin films thicker than monolayer, BiMnO_3 layers below the surface layer are the most bulk-like, but the Bi displacements are along the (111) direction and are parallel to each other. Interface with the substrate not only alters the direction of Bi off-center displacement, but also shifts the antiparallel pattern into a parallel one. Note that the (111) direction is the direction of Bi displacement in another multiferroic material, BiFeO_3 . Comparison between bulk BiMnO_3 and BiFeO_3 gives clearer hints on the differences between bulk and thin films of BiMnO_3 . BiFeO_3 exhibits a more ordered structure and its unit cell contains only two pseudo-cubic cells (eight cells for bulk BiMnO_3). Chemically the difference between BiMnO_3 and BiFeO_3 is the much weaker Jahn-Teller distortion in BiFeO_3 . The strong disorder in BiMnO_3 results from the competition between Jahn-Teller distortion around Mn ions and the off-center displacement of Bi ions. It is the Jahn-Teller distortion that drives the Bi ion displacement in (011) and antiparallel directions (FIG. 2 of Supplementary Material). In BiMnO_3 thin films the Bi ion displacements resemble those in BiFeO_3 because the interaction with the substrate reduces significantly the disorder in the Jahn-Teller distortions. Besides $\text{BiMnO}_3/\text{SrTiO}_3$ interfaces, surfaces of BiMnO_3 thin films also affect Bi ions displacements. While the Bi ions below the surface layer displace almost along the (111) direction, those in the surface layer displace along a direction between (111) and (001) directions.

Besides the spontaneous polarization mentioned above, a relatively low energy barrier for polarization rotation is another indicator of ferroelectricity. The energy barrier measures the external electric field strength required to rotate the direction of the polarization. The calculated energy barrier for a 90° rotation of the polarization is about 80 meV per BiMnO_3 formula unit (f.u.), a value that is 3 to 4 times larger than the 20 meV for BaTiO_3 [47], 30 meV for PbTiO_3 [48], and 25 meV in hexagonal RMnO_3 [49].

Next we turn to the valence states and magnetic moments of Mn ions. Charge disproportionation, the instability of Mn^{3+} valence states ($m = 3.7 \mu_B$) to form Mn^{2+} ($m = 4.5 \mu_B$) and Mn^{4+} ($m = 3.0 \mu_B$), occurs in BiMnO_3 thin films except the monolayer case. The valence states Mn^{2+} and Mn^{4+} always appear in pairs, and are not formed by charge transfer between BiMnO_3 thin films and the substrate. The density of states projected onto the SrTiO_3 substrate (not shown) shows that it remains insulating, so little charge transfer happens between the SrTiO_3 substrate and BiMnO_3 thin films. For a given pair, the Mn^{2+} ion resides in the surface layer and the

Mn^{4+} ion is located in the layer below it; they occupy the diagonal sites of one vertical face of a pseudo-cubic cell (see Supplementary Material Section III.B). The Mn-O bonds around the Mn^{2+} ion have different lengths: one is 2.45 Å and the other four are 2.05 Å. The six Mn^{4+} -O bonds have similar bond lengths of 1.90–2.00 Å. As a reference, for Mn^{3+} ions, two of Mn^{3+} -O bonds are between 2.15 and 2.25 Å, and the other four are between 1.90 and 2.00 Å. The volume occupied by Mn ions in different valence states is $\text{Mn}^{2+} > \text{Mn}^{3+} > \text{Mn}^{4+}$. The charge disproportionation thus introduces a local strain to the lattice, which explains the occurrence of Mn^{2+} - Mn^{4+} pairs only at the surface.

The occurrence of Mn^{2+} at the surface was observed in other perovskite manganites [50, 51]. Two possible mechanisms were proposed in the literature; one was attributed to the instability of Mn^{3+} via $2\text{Mn}^{3+} \rightarrow \text{Mn}^{2+} + \text{Mn}^{4+}$ [50], while ref. [51] proposed that Mn^{2+} ions result from chemical reduction by electron-doping or removing surface oxygens. The second mechanism may apply for the BiMnO_3 thin films, since Mn ions at the surface are bonded to five oxygens instead of six in the bulk. However this fails to explain the absence of Mn^{2+} in monolayer BiMnO_3 thin film. Electron-doping can be excluded because BiMnO_3 thin films with Mn^{2+} ions are still insulating. Nevertheless, the observation that Mn^{2+} and Mn^{4+} always occur in pairs support the Mn^{3+} instability mechanism. The local strain introduced by spontaneous charge disproportionation sheds light on understanding the difficulty during the experimental synthesis of BiMnO_3 thin films.

The charge disproportionation of Mn ions is manifested in their projected density of states (PDOS). In Fig. 3, we compared the PDOS on d -orbitals of Mn^{3+} ions in bulk C2/c BiMnO_3 and Mn^{3+} , Mn^{2+} , and Mn^{4+} ions in bilayer BiMnO_3 thin films. The d -shells of Mn^{2+} , Mn^{3+} and Mn^{4+} are d^5 , d^4 , and d^3 respectively. Due to Hund's rule, all the d -electrons occupy the same spin channel. The crystal field around Mn ions splits the 10 d -orbitals into triply degenerate t_{2g} and doubly degenerate e_g orbitals. The two e_g orbitals further split due to Jahn-Teller distortions. The four d -electrons of Mn^{3+} ions in bulk BiMnO_3 [Fig. 3(a)] are mainly located between -8 eV and -6 eV . The PDOS between -6 eV and -1 eV is contributed by hybridizations with O- p orbitals, and the PDOS in the spin-up channel above the energy gap is contributed by $d_{x^2-y^2}$ orbitals. Ions Mn^{3+} in thin films [Fig. 3(b)] exhibit a PDOS very similar to that in bulk BiMnO_3 , as expected, but on the other hand Mn^{2+} and Mn^{4+} ions show a very different PDOS. All five of the d -orbitals of the Mn^{2+} ion are occupied. The peak in the PDOS in the Mn^{4+} spin-up channel (unoccupied) is contributed by t_{2g} orbitals.

Summary and outlook. First-principles simulations of BiMnO_3 thin films on SrTiO_3 substrates confirm the presence of ferroelectric order in monolayer, bilayer, and

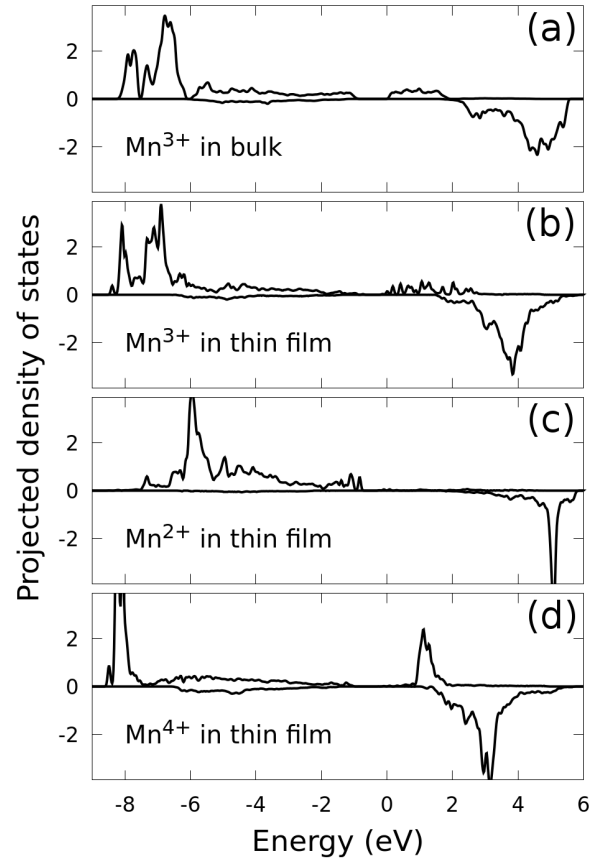


FIG. 3. Density of states projected onto Mn ions: (a) Mn^{3+} ions in bulk C2/c BiMnO_3 and (b) Mn^{3+} , (c) Mn^{2+} , (d) Mn^{4+} ions in bilayer BiMnO_3 thin film.

trilayer BiMnO_3 thin films. Our calculations show that these thin films are indeed multi-ferroic, that is, they exhibit both ferroelectric and magnetic behavior. The ferroelectricity originates from the ordered displacement of Bi ions from the tetrahedron centers, a consequence of the substrate constraint. Magnetic moments, density of states, and orbital analysis are presented to support our conclusions. We have resolved a long-standing physical problem of general interest and our observations point to a general principle in designing multiferroic materials by ordering dipole moments using substrate constraints. Hopefully this work will stimulate future experiments in search of multi-functional materials systems based on BiMnO_3 .

Acknowledgments. This work was supported by the US Department of Energy (DOE), Office of Basic Energy Sciences (BES), under Contract No. DE-FG02-02ER45995. Computations were done using the utilities of the National Energy Research Scientific Computing Center (NERSC).

* Corr. author: Hai-Ping Cheng, hping@ufl.edu

- [1] W. Eerenstein, N. D. Mathur, and J. F. Scott, *Nature* **442**, 759 (2006).
- [2] S.-W. Cheong and M. Mostovoy, *Nat. Mater.* **6**, 13 (2007).
- [3] R. Ramesh and N. A. Spaldin, *Nat. Mater.* **6**, 21 (2007).
- [4] J. Ma, J. Hu, Z. Li, and C.-W. Nan, *Advanced Materials* **23**, 1062 (2011).
- [5] N. A. Hill, *The Journal of Physical Chemistry B* **104**, 6694 (2000).
- [6] T. Atou, H. Chiba, K. Ohoyama, Y. Yamaguchi, and Y. Syono, *J. Solid State Chem.* **145**, 639 (1999).
- [7] A. Moreira dos Santos, A. K. Cheetham, T. Atou, Y. Syono, Y. Yamaguchi, K. Ohoyama, H. Chiba, and C. N. R. Rao, *Phys. Rev. B* **66**, 064425 (2002).
- [8] A. A. Belik, S. Iikubo, T. Yokosawa, K. Kodama, N. Igawa, S. Shamoto, M. Azuma, M. Takano, K. Kimoto, Y. Matsui, and E. Takayama-Muromachi, *Journal of the American Chemical Society* **129**, 971 (2007).
- [9] E. Montanari, G. Calestani, L. Righi, E. Gilioli, F. Bolzoni, K. S. Knight, and P. G. Radaelli, *Phys. Rev. B* **75**, 220101 (2007).
- [10] C. C. Chou, S. Taran, J. L. Her, C. P. Sun, C. L. Huang, H. Sakurai, A. A. Belik, E. Takayama-Muromachi, and H. D. Yang, *Phys. Rev. B* **78**, 092404 (2008).
- [11] D. P. Kozlenko, A. A. Belik, S. E. Kichanov, I. Mirebeau, D. V. Sheptyakov, T. Strässle, O. L. Makarova, A. V. Belushkin, B. N. Savenko, and E. Takayama-Muromachi, *Phys. Rev. B* **82**, 014401 (2010).
- [12] T. Kimura, S. Kawamoto, I. Yamada, M. Azuma, M. Takano, and Y. Tokura, *Phys. Rev. B* **67**, 180401 (2003).
- [13] A. M. dos Santos, S. Parashar, A. Raju, Y. Zhao, A. Cheetham, and C. Rao, *Solid State Commun.* **122**, 49 (2002).
- [14] Z. Chi, H. Yang, S. Feng, F. Li, R. Yu, and C. Jin, *Journal of Magnetism and Magnetic Materials* **310**, e358 (2007).
- [15] F. Zavaliche, S. Y. Yang, T. Zhao, Y. H. Chu, M. P. Cruz, C. B. Eom, and R. Ramesh, *Phase Transitions* **79**, 991 (2006).
- [16] C. Lu, W. Hu, Y. Tian, and T. Wu, *Appl. Phys. Rev.*, **2**, 021304 (2015).
- [17] D. G. Schlom, L.-Q. Chen, C.-B. Eom, K. M. Rabe, S. K. Streiffer, and J.-M. Triscone, *Annu. Rev. Mater. Res.* **37**, 589626 (2007).
- [18] J. Y. Son, B. G. Kim, C. H. Kim, and J. H. Cho, *Appl. Phys. Lett.* **84**, 4971 (2004).
- [19] H. Jeon, G. Singh-Bhalla, P. R. Mickel, K. Voigt, C. Morien, S. Tongay, A. F. Hebard, and A. Biswas, *J. Appl. Phys.* **93**, 074104 (2011).
- [20] J. Y. Son and Y.-H. Shin, *Appl. Phys. Lett.* **93**, 062902 (2008).
- [21] A. Sharan, J. Lettieri, Y. Jia, W. Tian, X. Pan, D. G. Schlom, and V. Gopalan, *Phys. Rev. B* **69**, 214109 (2004).
- [22] G. M. D. Luca, D. Preziosi, F. Chiarella, R. D. Capua, S. Gariglio, S. Lettieri, and M. Salluzzo, *Appl. Phys. Lett.* **103**, 062902 (2013).
- [23] M.-H. Jung, I. K. Yang, and Y. H. Jeong, *J. Korean Physical Society* **63**, 624 (2013).
- [24] B. W. Lee, P. S. Yoo, V. B. Nam, K. R. N. Toreh, and C. U. Jung, *Nanoscale Res. Lett.* **10**, 47 (2015).
- [25] N. A. Hill and K. M. Rabe, *Phys. Rev. B* **59**, 8759 (1999).
- [26] P. Baettig, R. Seshadri, and N. A. Spaldin, *J. Am. Chem. Soc.* **129**, 9854 (2007).
- [27] A. J. Hatt and N. A. Spaldin, *Eur. Phys. J. B* **71**, 435 (2009).
- [28] D. W. Boukhvalov and I. V. Solovyev, *Phys. Rev. B* **82**, 245101 (2010).
- [29] J. A. McLeod, Z. V. Pchelkina, L. D. Finkelstein, E. Z. Kurmaev, R. G. Wilks, A. Moewes, I. V. Solovyev, A. A. Belik, and E. Takayama-Muromachi, *Phys. Rev. B* **81**, 144103 (2010).
- [30] F. Tran and P. Blaha, *Phys. Rev. Lett.* **102**, 226401 (2009).
- [31] X. H. Zhu, X. R. Chen, and B. G. Liu, *Solid State Communications* **243**, 65 (2016).
- [32] O. Diéguez and J. Íñiguez, *Phys. Rev. B* **91**, 184113 (2015).
- [33] E. Bousquet and N. Spaldin, *Phys. Rev. B* **82**, 220402 (2010).
- [34] L. de' Medici, *Phys. Rev. B* **83**, 205112 (2011).
- [35] L. de' Medici, J. Mravlje, and A. Georges, *Phys. Rev. Lett.* **107**, 256401 (2011).
- [36] H. Nakamura, N. Hayashi, N. Nakai, M. Okumura, and M. Machida, *Physica C: Superconductivity* **469**, 908 (2009).
- [37] T. A. Mellan, F. Corà, R. Grau-Crespo, and S. Ismail-Beigi, *Phys. Rev. B* **92**, 085151 (2015).
- [38] H. Yamada, Y. Ogawa, Y. Ishii, H. Sato, M. Kawasaki, H. Akoh, and Y. Tokura, *Science* **305**, 646 (2004).
- [39] A. Ohtomo and H. Y. Hwang, *Nature* **427**, 423 (2006).
- [40] H. Y. Hwang, *MRS Bulletin* **31**, 28 (2006).
- [41] J. Mannhart and D. G. Schlom, *Science* **327**, 1607 (2010).
- [42] A. F. Moreira dos Santos, A. K. Cheetham, W. Tian, X. Pan, Y. Jia, N. J. Murphy, J. Lettieri, and D. G. Schlom, *Appl. Phys. Lett.* **84**, 91 (2004).
- [43] C.-H. Yang, T. Y. Koo, S.-H. Lee, C. Song, K.-B. Lee, and Y. H. Jeong, *Europhys. Lett.* **74**, 348 (2006).
- [44] M. Salluzzo, S. Gariglio, D. Stornaiuolo, V. Sessi, S. Rusponi, C. Piamonteze, G. M. De Luca, M. Minola, D. Marré, A. Gadaleta, H. Brune, F. Nolting, N. B. Brookes, and G. Ghiringhelli, *Phys. Rev. Lett.* **111**, 087204 (2013).
- [45] R. Seshadri and N. A. Hill, *Chem. Mater.* **13**, 28922899 (2001).
- [46] B. Silvi and A. Savin, *Nature* **371**, 683 (1994).
- [47] R. E. Cohen and H. Krakauer, *Phys. Rev. B* **42**, 6416 (1990).
- [48] U. V. Waghmare and K. M. Rabe, *Phys. Rev. B* **55**, 6161 (1997).
- [49] Y. Kumagai and N. A. Spaldin, *Nature Communications* **4**, 1540 (2013).
- [50] M. F. Hundley and J. J. Neumeier, *Phys. Rev. B* **55**, 11511 (1997).
- [51] S. Valencia, A. Gaupp, W. Gudat, L. Abad, L. Balcells, A. Cavallaro, B. Martínez, and F. J. Palomares, *Phys. Rev. B* **73**, 104402 (2006).